

A photoluminescence study of $\text{CdS}_x\text{Se}_{1-x}$ semiconductor quantum dots

This article has been downloaded from IOPscience. Please scroll down to see the full text article.

1992 J. Phys.: Condens. Matter 4 7521

(<http://iopscience.iop.org/0953-8984/4/36/023>)

View [the table of contents for this issue](#), or go to the [journal homepage](#) for more

Download details:

IP Address: 171.66.16.96

The article was downloaded on 11/05/2010 at 00:32

Please note that [terms and conditions apply](#).

A photoluminescence study of $\text{CdS}_x\text{Se}_{1-x}$ semiconductor quantum dots

Guang Mei†

Physics Department and Center for Integrated Electronics, Rensselaer Polytechnic Institute, Troy, NY 12180, USA

Received 31 March 1992, in final form 7 July 1992

Abstract. We report a study of room temperature photoluminescence, electromodulation and Raman scattering experiments on $\text{CdS}_x\text{Se}_{1-x}$ quantum dots of various sizes (18 Å to 108 Å) embedded in a glass matrix. The Raman experiment confirms that all the samples have the same semiconductor composition. Electromodulation is used to identify the quantum confinement peak position. The observed peaks of photoluminescence and electromodulation spectra are not at the same position and the difference is dependent on the particle size. An explanation in terms of a bound exciton is given to interpret the photoluminescence spectra.

1. Introduction

$\text{CdS}_x\text{Se}_{1-x}$, CdS and CdSe semiconductor nanocrystallites, or quantum dots (diameter less than 20 nm) embedded in an insulating material have attracted increasing attention in the past few years due to their fundamental quantum confinement properties as well as potential applications in optical devices [1-5]. Studies of their electronic and optical properties have been made extensively, using techniques such as optical absorption, photomodulation (PM), Raman scattering, electromodulation (EM) and photoluminescence (PL) [1-24]. The absorption spectrum has been used most often to show the quantum confinement structure of the semiconductor nanocrystallite because it can be observed easily at room temperature. PM studies such as pump-probe experiments were carried out to study the electronic transition between quantized energy levels and other associated processes in quantum dots. The Raman scattering technique was also used to determine the semiconductor composition in $\text{CdS}_x\text{Se}_{1-x}$ nanocrystallite [7] and to study the electron-phonon interaction [17]. Recently the EM technique was also applied to resolve the quantized energy levels precisely [25, 26]. PL experiments, however, being among the most straightforward probing techniques and complementary to other methods, have been widely used to study the quantum confinement structure and deep-level trap states in $\text{CdS}_x\text{Se}_{1-x}$ quantum dots.

Recently experiments done by Hache *et al* [14] showed that the PL spectrum at 77 K for $\text{CdS}_x\text{Se}_{1-x}$ quantum dots embedded in a glass matrix exhibits three peaks, a broad one located well below the semiconductor band edge and two narrow ones

† Present address: W M Keck Laboratory, Department of Chemistry, New York University, New York, NY 10003, USA.

close to the absorption edge. The broad peak is attributed to the recombination from deep trap levels in the gap. The explanation given for the two narrow peaks (50–100 meV apart) was that one is due to direct electron–hole recombination and the other, with slightly lower energy, is due to surface states. PL experiments done by others at room temperature [18, 19, 22, 23] and at low temperature [9, 10, 12, 16, 21, 24] normally show two peaks, a narrow peak near the semiconductor absorption edge and a broad band that is located well below the semiconductor band edge. The narrow peak is assigned to a direct recombination process of an electron and hole or a weakly bound exciton, and its position and shape are sensitive to the particle size [8, 10], semiconductor composition [20] and laser pumping flux [10]. Bawendi *et al* [15] claimed that the luminescence properties of CdSe quantum dots are due to the mixing of interior and localized surface states. It is interesting to note that all the above PL spectra of $\text{CdS}_x\text{Se}_{1-x}$ quantum dots (obtained for various particle sizes and at different temperatures) show that the position of the narrow peak near the band edge is not at the same position as the first-quantized optical transition level or quantum confinement peak position which has been observed in absorption spectrum. According to the principle of detailed balance, PL is closely linked to optical absorption. If the photon excitation only changes the occupation of states, with no change in the electronic structure of the particle (single-particle, rigid-band model), then we would expect the PL peak position and the quantum confinement peak position to be the same. Furthermore, all the above experimental data show that the PL peak is lower in energy than the quantum confinement peak. Also, most of the reports only show results for one dot size. In order to understand the origin of PL peaks in $\text{CdS}_x\text{Se}_{1-x}$ quantum dots better and to study the possible effect of the surface states or trap states on PL, it is important to study the PL spectrum with various dot sizes, because presumably the effect due to surface states would depend on the dot size.

In this paper, we make $\text{CdS}_x\text{Se}_{1-x}$ quantum dots of various sizes by heat treatment and annealing processes. A Raman experiment is performed to determine the composition of these samples. Both absorption and EM are used to identify the quantum confinement peak. PL spectroscopy measurements are carried out to study the origin of the PL narrow peak and the surface states. From comparing the absorption, EM and PL spectrum, we propose that the PL peak near the band edge is due to the bound exciton in quantum dots.

2. Experimental details

Samples were prepared from commercially available (1 mm thick, polished) Schott RG630 filter glass. A single as-received filter was cut into pieces and remelted in an oven at about 1000 °C and then quenched to room temperature. The sample was then annealed at 550 °C to initiate nucleation and at 600 °C to 655 °C for various times (from 30 to 360 minutes) to grow crystals. The above annealing temperature and sequence were established in order to maximize the crystal volume fraction. By varying the annealing temperature and growth time, we obtained a series of samples with varying average crystallite sizes. Structural and optical measurements were carried out on pieces of the same sample.

The average crystallite diameter was determined using dark- and bright-field transmission electron microscopy (TEM). The samples were polished down to about 30 μm

in thickness, ion milled and then carbon coated before direct examination by TEM. Several samples with average crystallite sizes ranging from 18 Å to 108 Å in diameter were used in the experiments. The measurement results are listed in table 1. A typical TEM picture is shown in figure 1 (sample C13).

Table 1. Synopsis of measurements of $CdS_{0.44}Se_{0.56}$ semiconductor nanocrystals.

Sample	Average radius (Å)	Standard deviation (Å)	EM peak position E_1 (eV)	PL peak position E_2 (eV)	Peak shift (meV)
C2	—	—	2.49	2.34	150
C13	9	3	2.34	2.23	110
C3	31	7	2.22	2.15	70
RG630	54	19	2.05	2.00	50

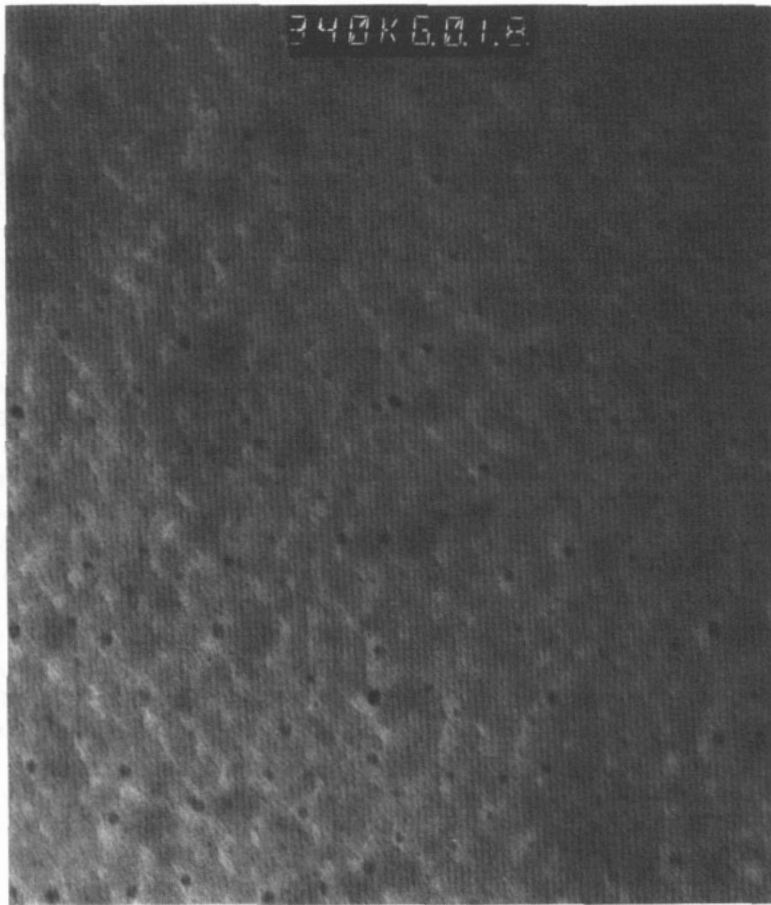


Figure 1. A TEM image for sample C13.

The crystallite composition was determined using Raman scattering: a Raman determination of the composition was made using the optic-mode peak spacing between CdS and CdSe-like modes [7].

The absorption coefficient α was measured using a Cary Model 17 dual-beam spectrophotometer. Electromodulation experiments were carried out using a 0.5 m Spex 1600 monochromator coupled to a THORN EMI photomultiplier (type 9659B). An AC voltage of about 500 V (RMS) was applied across a thin sample ($\approx 100 \mu\text{m}$ in thickness) yielding an RMS field of 10^4 V cm^{-1} in the particles. The in-phase modulation source was chopped (at about 1 kHz) and the modulation in the signal at twice the modulation frequency was detected with a lock-in amplifier. The unmodulated transmission was also measured by a multimeter.

All PL measurements reported here were pumped with a chopped Ar laser operated at 488 nm, which is well above the semiconductor absorption edge for all samples. The chopper frequency was kept at about 1500 Hz in order to reduce the stray noise. The signal was collected by a lens and focused into a 0.5 m Spex 1600 monochromator coupled to a photomultiplier. The signal then was picked up by a lock-in amplifier.

All the above experiments were done at room temperature.

3. Results

Figure 2 illustrates the Raman spectra for the original RG630 and annealed samples C3, C13 and C2. Two clear modes corresponding to CdS and CdSe longitudinal optic modes were observed. The difference between the peak positions for the CdS-like mode and the CdSe-like mode was $83 \pm 2 \text{ cm}^{-1}$ for all the samples. The composition of the samples was characterized using the difference in position between the two peaks. The composition was the same for all samples with $x = 0.44 \pm 0.01$. We note that this result means that the composition of crystallites does not change substantially during crystal growth. Hence the differences of absorption edges of samples C2, C13, C3 and RG630 are solely due to the quantum confinement effect, because a 0.01 change of composition x corresponds to a change of only 8 meV in the energy gap (or, alternatively, 65 cm^{-1}).

In figure 3 we show the absorption coefficient α plotted on a logarithmic scale against photon energy for all the samples. The absorption edge, defined here by extrapolating α^2 against photon energy, is 2.34 eV (for C2), 2.23 eV (for C13), 2.14 eV (for C3) and 2.00 eV (for RG630), respectively. Relatively little quantum structure is seen for RG630 because the particles are large ($\geq 100 \text{ \AA}$ in diameter) and there is a relatively broad particle size distribution [6]. Peaks that might be associated with quantum confinement are observed for C3, C13 and C2 due to the smaller average particle diameters of 62 \AA (for C3) and 18 \AA (for C13) of the samples (for C2 the size is even smaller, although no TEM has been performed because of the resolution limit of 5 \AA of the microscope).

Room temperature EM spectra are shown in figure 4. The magnitude of $\Delta T/T$ (T is transmission) varies linearly as the field squared, and the position and shape of the modulation spectrum does not vary with field, confirming that the EM is due to the Stark effect [27–29]. The modulation spectrum consists of two induced transmission peaks which are due to spin-orbit splitting [30]. The resolved EM peak positions E_1 are listed in table 1. The shift of the first-quantized energy level for the optical

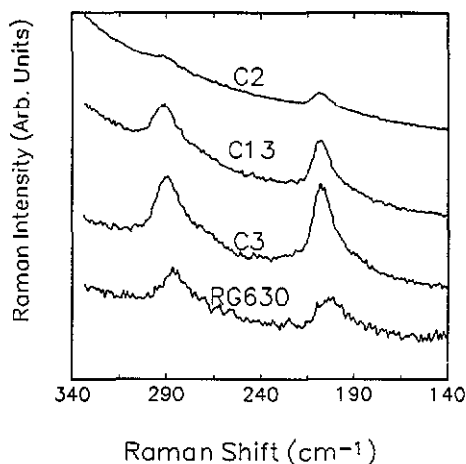


Figure 2. The Raman-scattered intensity plotted against the Raman shift for C2, C13, C3 and RG630. The excitation wavenumber is 19436 cm^{-1} (514.5 nm).

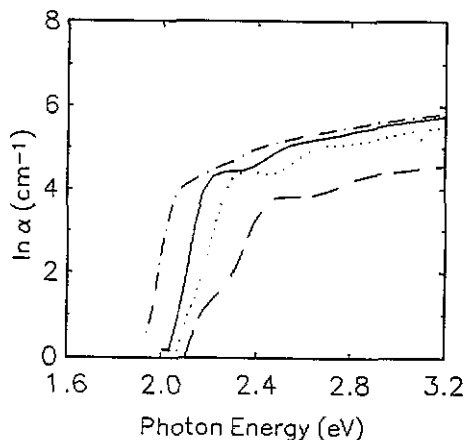


Figure 3. The optical absorption coefficient α plotted against the photon energy for C2, C13, C3 and RG630 at room temperature. Note the logarithmic scale. Long dash: C2; dots: C13; solid line: C3; dot dash: RG630.

transition due to the external electrical field gives rise to the oscillating feature of the $\Delta\alpha$ spectrum. Here the observed spectrum is broadened by the particle size distribution and other broadening mechanisms such as thermal broadening. In this paper, we use the EM spectrum to locate quantized energy levels. The applied external electrical field tilts the potential well, resulting in a reduction of wavefunction overlap and hence in the transition probability of the unperturbed quantized energy level. Therefore, the peak position of the EM spectrum should be the same as that of the absorption spectrum [26–30]. From figures 3 and 4 we can see that they agree very well, but the quantized energy level can be measured more precisely using the EM technique.

In figure 5 we show the room temperature PL spectra for samples RG630, C3, C13 and C2. A peak is observed at 2.00 eV for RG630, 2.15 eV for C3, 2.23 eV for C13 and 2.34 eV for C2, close to their extrapolated band gaps respectively. We note that the PL peak position is lower than the first quantum confinement peak for all the samples we study here. A broader band appears for the annealed samples that is believed to be due to large number of surface states or trap states below the band edge.

4. Discussion

As we mentioned in the last section, the Raman experiment confirms that all the samples have the same semiconductor composition, so the difference in absorption peak position is solely due to the quantum confinement effect. In the EM experiment, the absorption peak positions would shift due to the applied electric field, and the oscillator strength of the absorption at the quantum confinement peak position decreases, since the overlap of the electron and hole wavefunctions is smaller. Also,

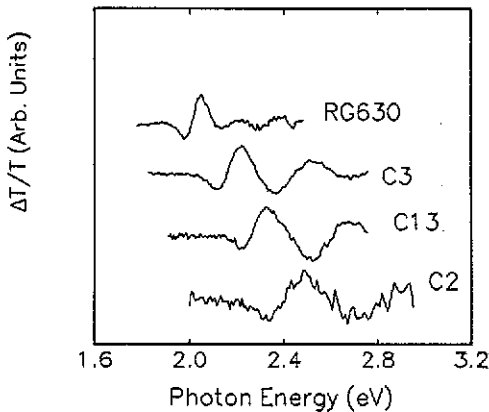


Figure 4. EM spectra; the relative change of transmission $\Delta T/T$ (in arbitrary units) plotted against the photon energy for RG630, C3, C13 and C2.

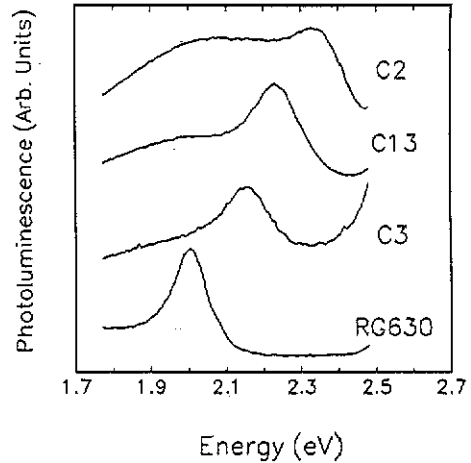


Figure 5. PL spectra; the intensity plotted against the photon energy for C2, C13, C3 and RG630.

a new transition would appear because the loss of absorption strength in allowed transitions is compensated by the appearance of absorption strengths in previously forbidden transitions. This gives rise to the oscillating feature of the EM spectrum. Thus the positive peak position of $\Delta T/T$ gives the previously allowed transition level, i.e. the quantum confinement peak position. These peaks are precisely resolved by EM and can be used for comparison with PL spectra.

The analysis of the PL is based on the principle of detailed balance which uses the fact that the coupling of a transition between two states to an external field is symmetric in time. This means that the spontaneous emission cross section is equal to the absorption cross section for a given transition [31]. Then we would expect the quantum confinement peak position and PL peak position to be identical. As we see in table 1, there is a shift between them and the shift also depends on the particle size, ranging from 50 meV for RG630 to 150 meV for C2. This indicates that the PL peak is due to bound-exciton recombination, related to impurity or surface states of $\text{CdS}_x\text{Se}_{1-x}$ quantum dots. That is, the narrow PL peak does not correspond to the direct electron-hole interband recombination but to carrier recombination through other levels such as surface states or other trap states [18]. This argument is indirectly supported by the PL spectrum—more and more surface states appear in the spectrum when the particle size gets small (the PL broad band below the absorption edge). We can see in figure 5 that the ratio of the intensity of the broad band to that of the narrow peak near the band edge increases when the particle size decreases. This result is also observed in other PL experiments [14]. The existence of surface states is in fact very important for explaining the mechanism of photoinduced changes of absorption [29, 32].

Another possible explanation for a PL peak shift towards a lower energy level, as compared with the quantum confinement peak, is that it occurs because of the phonon quantization in $\text{CdS}_x\text{Se}_{1-x}$ quantum dots. We do not believe this is the explanation because the quantized phonon energy is of the order of 30 meV in these

particles and the shift of more than 100 meV observed for sample C2 (radius = 9 Å) seems to be too large for this model to accommodate.

In summary, room temperature PL of $\text{CdS}_x\text{Se}_{1-x}$ quantum dots of various sizes embedded in a glass matrix has been studied. From careful comparison with the EM spectrum, which is a sensitive probe of the quantum confinement peak, the origin of the narrow PL peak near the absorption edge has been identified as being due to a bound exciton.

Acknowledgments

The author is grateful to Professor P D Persans for many helpful discussions, S Carpenter for some sample preparation work and Dr L E Felton for TEM measurements. This work was supported in part by the NSF under grant number DMR-9104086 and by the Optoelectronics Technology Center funded by DARPA.

References

- [1] Brus L E 1983 *J. Chem. Phys.* **79** 5566
- [2] Brus L E 1984 *J. Chem. Phys.* **80** 4403
- [3] Tsuda S and Cruz C H B 1991 *Opt. Lett.* **16** 1597
- [4] Hall D W and Borrelli N F 1988 *J. Opt. Soc. Am.* **B 5** 1650
- [5] Persans P D, Tu An, Wu Y-J and Lewis M 1989 *J. Opt. Soc. Am.* **B 6** 818
- [6] Persans P D, Tu An, Lewis M, Driscoll T and Redwing R 1990 *Mater. Res. Soc. Symp. Proc.* **164** 105
- [7] Tu An and Persans P D 1991 *Appl. Phys. Lett.* **58** 1506
- [8] Inokuma T, Arai T and Ishikawa M 1990 *Phys. Rev.* **42** 11 093
- [9] Potter B G Jr and Simmons J H 1988 *Phys. Rev.* **B 37** 10 838
- [10] Ekimov A I, Kudryavtsev I A, Ivanov M G and Efros Al L 1989 *Sov. Phys.-Solid State* **31** 1385; 1990 *J. Lumin.* **46** 83
- [11] Bugayev A, Kalt H, Kuhl J and Rinker M 1991 *Appl. Phys. A* **53** 75
- [12] Misawa K, Yao H, Hayashi T and Kobayashi T 1991 *Chem. Phys. Lett.* **183** 113
- [13] Burkitbaev S, Bertolotti M, Fazio E, Ferrari A, Liakhov G and Sibilia C 1992 *J. Appl. Phys.* **71** 941
- [14] Hache F, Klein M C, Ricard D and Flytzanis C 1991 *J. Opt. Soc. Am.* **B 8** 1802
- [15] Bawendi M G, Carroll P J, Wilson W L and Brus L E 1992 *J. Chem. Phys.* **96** 946
- [16] Ermolovich I B, Kulish N R, Kunets V P, Lisitsa M P, Malysh N I and Sheinkman M K 1990 *Opt. Spectrosc.* **68** 499
- [17] Alivisatos A P, Harris T D, Carroll P J, Steigerwald M L and Brus L E 1989 *J. Chem. Phys.* **90** 3463
- [18] Shinjima H, Yumoto J, Uesugi N, Omi S and Asahara Y 1989 *Appl. Phys. Lett.* **55** 1519
- [19] Borrelli N F, Hall D W, Holland H J and Smith D W 1987 *J. Appl. Phys.* **61** 5399
- [20] Tu An and Persans P D unpublished data
- [21] Bawendi M G, Wilson W L, Rothberg L, Carroll P J, Jedju T M, Steigerwald M L and Brus L E 1990 *Phys. Rev. Lett.* **65** 1623
- [22] Andrianasolo B, Champagnon B, Ferrari M and Neuroth N 1991 *J. Lumin.* **48 & 49** 306
- [23] Rodden W S O, Sotomayor Torres C M, Ironside C N, Cotter D and Girdlestone H P 1991 *Superlatt. Microstruct.* **9** 421
- [24] Uhrig A, Banyai L, Gaponenko S, Worner A, Neuroth N and Klingshirn C 1991 *Z. Phys.* **D 20** 345
- [25] Nomura S and Kobayashi T 1990 *Solid State Commun.* **73** 425
- [26] Mei Guang, Carpenter S, Felton L E and Persans P D 1992 *J. Opt. Soc. Am.* **B** at press
- [27] Henneberger F, Puls J, Rossmann H, Woggon U, Freundt S, Spiegelberg Ch and Schulzgen A 1990 *J. Cryst. Growth* **101** 632
- [28] Ekimov A I, Efros Al L, Shubina T V and Skvortsov A P 1990 *J. Lumin.* **46** 97
- [29] Mei Guang, Persans P D and Tu A 1991 *Mater. Res. Soc. Symp. Proc.* **206** 145

- [30] Hache F, Ricard D and Flytzanis C 1989 *Appl. Phys. Lett.* **55** 1504
- [31] Rose A 1963 *Concepts in Photoconductivity and Allied Problems* (New York: Interscience)
- [32] Mei Guang, Carpenter S and Persans P D 1991 *Solid State Commun.* **80** 557